JTE HCMUTE
ISSN: 2615-9740

JOURNAL OF TECHNICAL EDUCATION SCIENCE
Ho Chi Minh City University of Technology and Education
Website: https://jte.edu.vn
Email: jte@hcmute.edu.vn

# Fabrication of Bio-Composites From Sugarcane Bagasse Cellulose and Poly(Lactic Acid)

**Nguyen Hong Nhu Pham[1], Van Tai Pham[1], Phuong Dong Bui[1], Thanh Huy Nguyen[2], Bui Anh Duy Nguyen[2], Thi Thuy Giang Bach[3], Chi Thanh Nguyen[1*]**

*[1]Ho Chi Minh City University of Technology and Education, Vietnam*
*[2]Ho Chi Minh City University of Technology (HCMUT), VNU-HCM, Vietnam*
*[3]Nong Lam University, Ho Chi Minh City, Vietnam*

[*]Corresponding author. *Email: thanhnc@hcmute.edu.vn*

**ARTICLE INFO**

Received: 14/09/2025
Revised: 02/10/2025
Accepted: 13/10/2025
Published: 28/11/2025

**KEYWORDS**

Agricultural biomass;
Sugarcane bagasse;
Cellulose fibers;
Bio-composite;
Polylactic acid.

**ABSTRACT**

The development trend of green materials based on agricultural waste combined with biodegradable polymers such as PLA, PVA, starch, and chitosan has significantly advanced in recent decades. This trend was driven by the rapid increase in plastic waste and agricultural biomass, which have had substantial negative impacts on the environment and human health. This study aimed to extract cellulose fibers from sugarcane bagasse as a reinforcing agent for PLA-based bio-composites. Scanning electron microscopy (SEM) analysis results showed that the extracted cellulose fibers had smooth surfaces and were relatively well dispersed in the PLA matrix. Infrared spectroscopy (FTIR) analysis technique showed that the chemical structure of cellulose fibers unchanged after chemical treatment and the effective removal of amorphous components. X-ray diffraction analysis showed a type I cellulose crystalline structure of the extracted cellulose fibers with a crystallinity index of 63.71%. Thermal gravimetric analysis identified three stages of weight loss for the extracted cellulose fibers: below 120 ºC, from 120 ºC to 380 ºC, and above 380 ºC. The analysis results of mechanical properties of bio-composites indicated that upon incorporation of cellulose at loading ranging from 0.1% to 0.5%, the mechanical performance of the bio-composites decreased compared to that of neat PLA.

Doi: https://doi.org/10.54644/jte.2025.2002



## 1. Introduction

In recent years, the research and development of green materials derived from agricultural biomass were given considerable attention to mitigate the negative environmental impacts caused by the excessive use of virgin plastics. Polylactic acid (PLA) was identified as a biodegradable and biocompatible thermoplastic polyester [1]. PLA was synthesized through the ring-opening polymerization of lactic acid, which was fermented from renewable plant-based resources such as corn and potato starch [2]. This material was reported to exhibit outstanding properties and was applied in various industries including packaging, thermoplastics, textiles, and medicine [1]. However, PLA was limited by its high cost, brittleness, poor thermal stability, and high gas permeability, which restricted its wide applications [1-3]. Composites based on PLA reinforced with nanocellulose fibers were shown to significantly improve mechanical properties, water resistance, and biodegradability. These enhancements were mainly attributed to the large specific surface area of cellulose fibers and the strong interaction between the matrix and the reinforcement, as reported in previous studies [4], [5].

Among agricultural biomass sources, sugarcane bagasse represented one of the most common and abundant wastes. According to the Food and Agriculture Organization (FAO), global sugarcane production exceeded 1.9 billion tons in 2022, with Brazil accounting for 38% (approximately 725 million tons). In Vietnam, sugarcane production in 2022 reached more than 11 million tons [6]. Bagasse constituted about 30% of sugarcane by weight, meaning that nearly 600 million tons of bagasse were generated globally in 2022 [7]. Most bagasse was mainly treated by burning, with a smaller proportion

used as fuel for power generation and as animal feed [8]. Therefore, bagasse had not been effectively utilized. Previous studies reported that bagasse contained 35–50% cellulose [9], which was higher than other agricultural residues such as corn cob (33.7 wt%), wheat straw (32.9 wt%), rice straw (36.2 wt%), and corn stalk (35 wt%) [8]. In addition to cellulose fibers, bagasse also contained hemicellulose (25–35 wt%), lignin (18–24 wt%), and other soluble components [10, 11]. These findings indicated that bagasse was an efficient biomass source for the production of nanocellulose fibers, contributing to sugarcane waste management and generating value-added materials.

Recently, cellulose fibers extracted from bagasse have been increasingly investigated as reinforcing agents in PLA matrices. Microcrystalline cellulose derived from bagasse was reported to be uniformly dispersed in PLA, maintaining its chemical structure after treatment, and significantly improving thermal and mechanical properties at 5 wt%, with a decomposition temperature of 326.35 °C and a 50.98% increase in tensile strength compared to neat PLA [3]. Similarly, PLA nanocomposite films reinforced with bagasse-derived nanocellulose achieved uniform dispersion and the highest crystallinity at 2 wt%. The reinforced films exhibited a higher contact angle (76.1° vs. 57.9° for neat PLA) and improved barrier performance [12].

In this study, cellulose fibers were extracted successfully from abundant agricultural and food processing by-products available in Vietnam, such as sugarcane bagasse via a simple, environmentally friendly method that avoids the use of hazardous chemicals. The extracted cellulose was subsequently combined with the eco-friendly polymer poly(lactic acid) to fabricate bio-composites in the form of bioplastic films. The resulting materials not only contribute to reducing organic and plastic waste but also provide significant economic value while positively impacting the environment. The fabricated PLA/cellulose fiber-based bio-composite films have great potential for the application as a sustainable and environmentally friendly agricultural mulch film replacing the conventional petroleum-based polyethylene agricultural mulch film.

## 2. Materials and Methods

### *2.1. Materials*

Sugarcane bagasse (SB) was collected in Ho Chi Minh City, Vietnam. Polylactic acid (PLA) 4043D was supplied by NatureWorks (Minnetonka, USA) with a molecular weight of approximately 110,000 g/mol. Sodium hydroxide (NaOH), hydrogen peroxide ($H_2O_2$), chloroform ($CHCl_3$), and acetone ($C_3H_6O$) were purchased from Sigma-Aldrich.

### *2.2. Isolation of cellulose from sugarcane bagasse*

Sugarcane bagasse was collected, cleaned to remove impurities, ground, sieved through a 60-mesh screen, and dried at 60 °C for 24 h. The dried sample was then treated with an alkaline–peroxide solution consisting of 4% NaOH and 10% $H_2O_2$ (v/v = 1:1) at a solid-to-liquid ratio of 1:25 (w/v) for 3 h. The solid fraction obtained after the reaction was filtered, washed with distilled water until neutral pH, and dried to yield bleached fibers. Subsequently, the fibers were treated with $H_2O_2$ solution at a solid-to-liquid ratio of 1:20 (w/v) at 70 °C for 3 h. After the reaction, the sample was centrifuged five times with distilled water at 6000 rpm for 10 min, followed by ultrasonication at 75 W for 15 min to obtain a cellulose suspension (CFs). To prevent microbial contamination, one drop of $CHCl_3$ was added prior to storing the suspension at 4 °C.

### *2.3. Preparation of cellulose suspension in acetone*

The aqueous cellulose suspension was centrifuged at 6000 rpm for 10 min to remove water. Acetone was then added to the solid residue, followed by centrifugation. This acetone centrifugation process was repeated three times to completely remove residual water. The final solid was re-dispersed in acetone and ultrasonicated at 75 W for 10 min to obtain a cellulose suspension in acetone.

### *2.4. Preparation of bio-composites*

PLA pellets were dissolved in chloroform to prepare a 3% (w/v) PLA solution, which was magnetically stirred at 40 °C for 2 h until completely dissolved. The cellulose suspension in acetone was then added dropwise at varying cellulose loadings and the mixture was further stirred for 1 h. The

resulting mixture was cast into Petri dishes and left to evaporate the solvent at room temperature to form PLA/CFs bio-composites.

### *2.5. Characterization*

#### *2.5.1. Fourier Transform Infrared Spectroscopy (FTIR)*

The chemical structures of sugarcane bagasse and cellulose fibers were analyzed using Fourier transform infrared (FTIR) spectroscopy (NICOLET 6700 spectrometer, University of Finance and Marketing, Ho Chi Minh City, Vietnam) over the wavenumber range of 4000–400 $cm^{-1}$ with a resolution of 2 $cm^{-1}$. The samples were prepared in pellet form by mixing the dried powders with KBr.

#### *2.5.2. Scanning Electron Microscopy (SEM)*

The surface morphology of sugarcane bagasse, cellulose fibers, and PLA/CFs composites was examined using a scanning electron microscope (SEM, HITACHI S-4800, Japan) at the R&D Center, Saigon Hi-Tech Park, with an accelerating voltage of 20 kV. The samples were mounted on metal stubs using carbon tape and coated with a thin platinum (Pt) layer prior to analysis.

#### *2.5.3. X-ray Diffraction (XRD)*

X-ray diffraction (XRD) analysis was performed to determine the crystalline structure of raw sugarcane bagasse and the extracted cellulose fibers. In this study, the samples were analyzed using an EMPYREAN diffractometer (PANalytical, Netherlands) at the University of Finance and Marketing, Ho Chi Minh City, Vietnam. The measurements were carried out over a scanning range of 5–80° (2θ) with CuKα radiation (λ = 1.54056 Å) at 30 kV and 45 mA. The crystallinity index (CI) of sugarcane bagasse and cellulose fibers was calculated according to Eq. (1) below [13]:

$$CI\ (\%) = \frac{(I_{200} - I_{am})}{I_{200}} \times 100 \quad (1)$$

where, $I_{200}$ represents the maximum intensity of the (200) diffraction peak and $I_{am}$ corresponds to the intensity of the amorphous region.

#### *2.5.4. Thermogravimetric Analysis (TGA)*

The thermal stability of raw sugarcane bagasse and cellulose fibers was determined using a Swiss Mettler Toledo TGA/DSC 3+ instrument at the Institute of Applied Materials Science, Vietnam. All samples were heated from 25 to 800 °C at a heating rate of 10 °C/min under a nitrogen atmosphere. Temperature and mass calibrations were performed prior to testing.

#### *2.5.5. Differential Scanning Calorimetry (DSC)*

The thermal properties of the bio-composites were analyzed using a Swiss Mettler Toledo TGA/DSC 3+ instrument at the Institute of Applied Materials Science, Vietnam. All samples were heated from 25 to 250 °C at a heating rate of 10 °C/min under a nitrogen atmosphere.

#### *2.5.6. Mechanical Properties of Bio-composite*

The mechanical properties of the bio-composites were evaluated according to ASTM D882. Rectangular specimens with a gauge length of 125 mm and a width of 10 mm were tested at a crosshead speed of 12.5 mm/min. The measurements were carried out using a SHIMADZU AGS-X universal testing machine (SHIMADZU, Japan) at the Laboratory of Materials Technology, Ho Chi Minh City University of Technology and Education, Vietnam. Each test was repeated five times, and the average values were reported.

#### *2.5.7. Water Absorption Capacity*

The water absorption capacity of the bio-composites was determined according to the method described in a published study [14], with slight modifications. Bio-composite specimens were cut into 2 × 2 cm squares and dried at 50 °C until a constant weight ($m_0$) was obtained. The dried samples were then immersed in distilled water at room temperature for 24 h. After surface moisture was removed, the samples were weighed again ($m_1$). The water absorption ratio (%) was calculated using Eq. (2):

$$\text{Water Absorption (\%)} = \frac{m_1 - m_0}{m_0} * 100 \quad (2)$$

where $m_0$ is the initial dry weight of the sample (g), and $m_1$ is the weight of the sample after immersion (g).

## 3. Results and Discussion

### *3.1. Scanning Electron Microscopy (SEM) of SB and CFs*

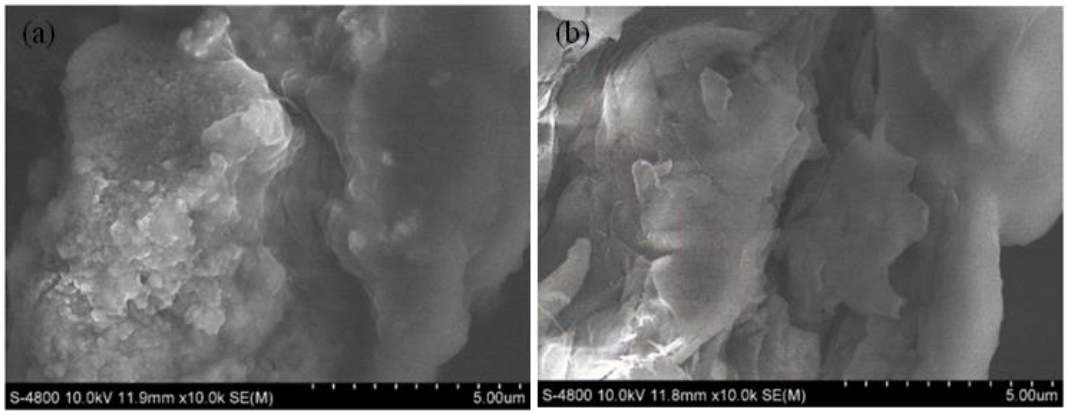


**Figure 1.** *SEM images of (a) SB; (b) CFs.*

The surface morphology of SB and CFs was analyzed using scanning electron microscopy (SEM), as shown in Figure 1. Observation in Figure 1a reveals that the surface of raw sugarcane bagasse exhibits a rough and heterogeneous structure due to the presence of hemicellulose, lignin, oil, and wax tightly bound together to form rigid fiber bundles [15]. In contrast, after chemical treatment, the surface of the cellulose fibers became smoother and more uniform (Figure 1b). This morphological change indicates that the chemical treatment effectively removed non-cellulosic components. These findings were consistent with a previous study [16].

### *3.2. Fourier Transform Infrared Spectroscopy (FTIR) of SB and CFs*

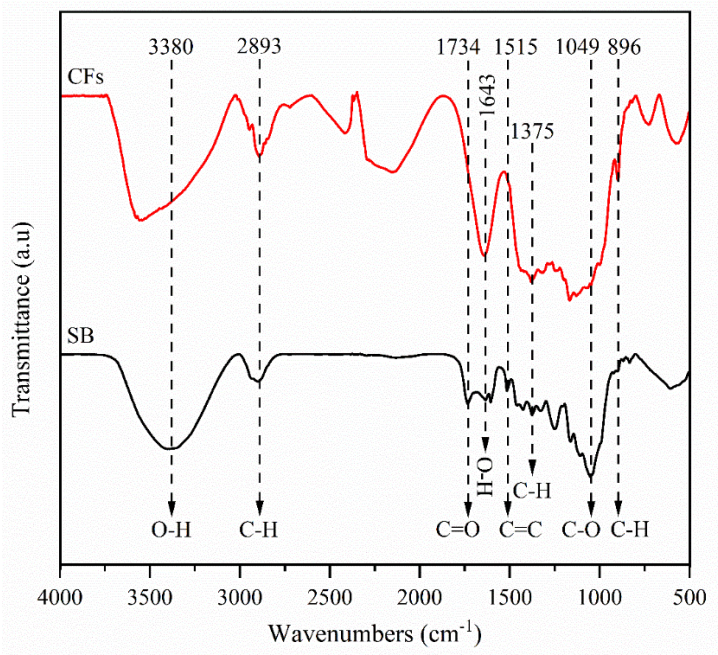


**Figure 2.** *The FTIR spectra of SB and CFs.*

The FTIR technique was employed to elucidate the functional group changes induced by chemical treatment [16]. The FTIR spectra of SB and CFs are presented in Figure 2. The results show that both

samples exhibit a broad band around 3385 $cm^{-1}$, attributed to the stretching vibration of hydroxyl (O–H) groups [17]. The absorption peak at 2899 $cm^{-1}$ corresponds to the stretching vibration of alkyl C–H groups in the aliphatic chain, while the band at 1730 $cm^{-1}$ is assigned to the stretching vibration of carbonyl (C=O) groups, characteristic of hemicellulose [18]. In addition, the appearance of the peak at 2419 $cm^{-1}$ was attributed to $CO_2$ vibrations, while the peak 2144 $cm^{-1}$ was assigned to C=C stretching vibrations. The occurrence of these two peaks can be explained by the lignin removal during the cellulose extraction process from sugarcane bagasse [19]. The peak at 1640 $cm^{-1}$ is attributed to the bending vibration of adsorbed water on hydrophilic groups [20]. Another important absorption band appears at 1517 $cm^{-1}$, assigned to (C=C) stretching vibrations in the lignin structure [15]. The simultaneous presence of a peak at 899 $cm^{-1}$ is attributed to the β-glycosidic linkages of glucose units. Notably, the characteristic peaks of hemicellulose (C=O) and lignin (C=C) disappeared in the FTIR spectrum of CFs, indicating that these two components were effectively removed after chemical treatment. Meanwhile, the fundamental chemical structure of cellulose was preserved. These results were consistent with the findings of a reported study [15].

### *3.3. X-ray Diffraction (XRD) of SB and CFs*

**Table 1.** *Crystallinity index of SB and CFs.*

| Samples | Crystallinity index (%) |
|---|---|
| SB | 24.41 |
| CFs | 63.71 |

The XRD patterns of SB and CFs are presented in Figure 3. For SB, the diffraction peaks appear relatively broad and less sharp, which is attributed to the presence of amorphous components such as hemicellulose and lignin, leading to a lower degree of structural order [9]. In contrast, the XRD pattern of CFs shows more distinct diffraction peaks at 2θ values of 15.88°, 22.08°, and 34.21°, corresponding to the (110), (200), and (004) planes of cellulose type I [21]. As shown in Table 1, the crystallinity index (CrI) of CFs reached 63.71%, which is significantly higher than that of raw SB (24.41%). This increase indicates that the chemical treatment effectively removed the amorphous regions, allowing cellulose chains to reorganize into a more ordered crystalline structure. Notably, a higher crystallinity value is often associated with enhanced thermal stability and improved mechanical properties. Similar results were also reported in another research [22], with CrI values of 35.67% for raw fibers and 77.89% for bleached fibers.

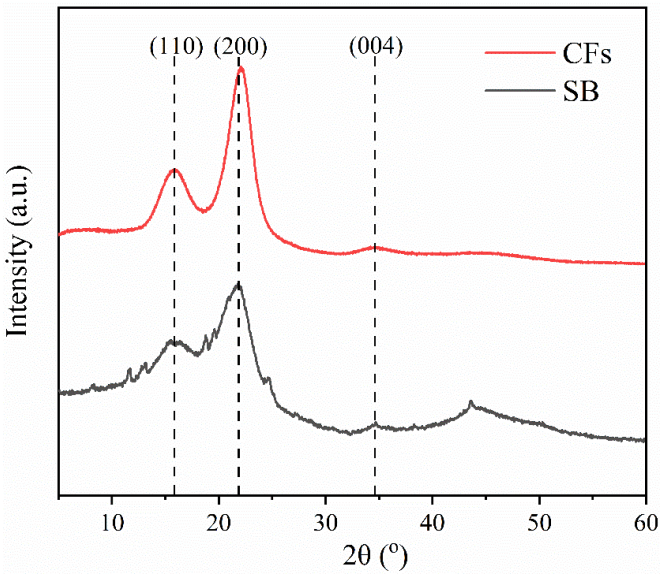


**Figure 3.** *XRD patterns of SB and CFs.*

### *3.4. Thermal properties of SB and CFs*

The thermal stability of SB and the obtained CFs was evaluated by thermogravimetric analysis (TGA), as shown in Figure 4. During this period a mass loss of the samples of about 4-5% was observed. This reduction was attributed to the evaporation of moisture, with a lower weight loss observed in cellulose fibers, indicating a lower residual moisture content after chemical treatment compared to bagasse. The subsequent stage occurred in the range of 120-400 °C and represented the main weight loss, with a reduction of about 62%. In this stage, hemicellulose and cellulose underwent decomposition. Hemicellulose degraded at a lower temperature, while cellulose decomposed at a higher range, but both contributed strongly to the overall mass loss. The final decomposition stage occurs when the temperature exceeds 380°C. At this stage, a mass loss of about 10%, mainly due to the decomposition of lignin. Lignin is a complex aromatic polymer and exhibited higher thermal stability than hemicellulose and cellulose. Its decomposition appeared at higher temperatures and extended over a broader range, leading to gradual weight loss in the last stage of thermal degradation. After chemical treatment, hemicellulose and lignin were removed effectively, resulting in improved crystallinity of the obtained cellulose fibers. This increase in crystallinity enhanced the thermal stability of cellulose fibers compared with sugarcane bagasse. The result was consistent with the XRD analysis presented in Figure 3. These results were consistent with previous studies [23], [24].

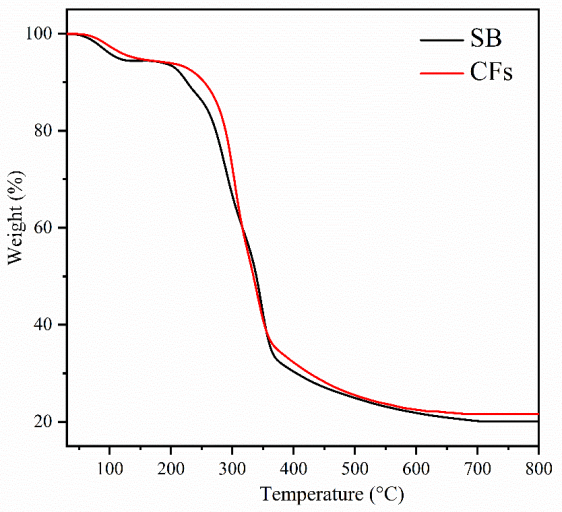


**Figure 4.** *TGA thermograph of SB and CFs.*

### *3.5. Scanning Electron Microscopy (SEM) of bio-composites*

The bio-composite material in this study was fabricated from cellulose and polylactic acid (PLA). Therefore, the properties of the bio-composites are strongly influenced by the interfacial interactions between the PLA matrix and the cellulose fiber reinforcement phase [25]. The morphological differences between the neat PLA and the PLA reinforced with 0.1% cellulose were examined using scanning electron microscopy (SEM), and the results are presented in Figure 5.

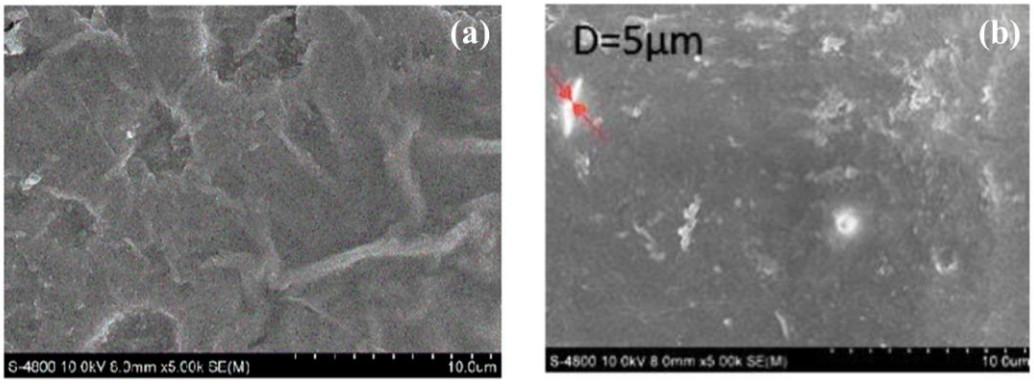


**Figure 5.** *SEM micrographs of (a) neat PLA and (b) PLA/0.1% cellulose.*

JTE
HCMUTE
ISSN: 2615-9740

JOURNAL OF TECHNICAL EDUCATION SCIENCE
Ho Chi Minh City University of Technology and Education
Website: https://jte.edu.vn
Email: jte@hcmute.edu.vn

The surface morphology of the neat PLA is shown in Figure 5(a). The micrograph reveals a relatively rough and uneven surface, with PLA fragments of varying sizes stacked irregularly. Such features likely contributed to the formation of voids and surface heterogeneity. This non-uniform morphology was partially improved upon the incorporation of cellulose fibers, as illustrated in Figure 5(b). The cellulose fibers, with an average diameter of approximately 5 µm, contributed to a smoother surface compared with that of the neat PLA. This observation was consistent with previous published researches [26], [27], which reported that PLA reinforced with acetylated cellulose fibers exhibited smoother surfaces and fewer defects than pristine PLA.

### *3.6. Differential Scanning Calorimetry (DSC) Analysis of bio-composite*

Neat PLA and PLA reinforced with cellulose fibers at different loadings (0.1%, 0.3%, and 0.5%) were subjected to differential scanning calorimetry (DSC) analysis. DSC provides insights into structural changes and crystallinity variations of polymers. The DSC thermograms of the samples are presented in Figure 6, while the corresponding thermal parameters including the glass transition temperature ($T_g$), crystallization temperature ($T_c$), melting temperature ($T_m$), and the enthalpies of crystallization ($\Delta H_c$), melting ($\Delta H_m$), as well as the degree of crystallinity ($X_c$) are summarized in Table 2.

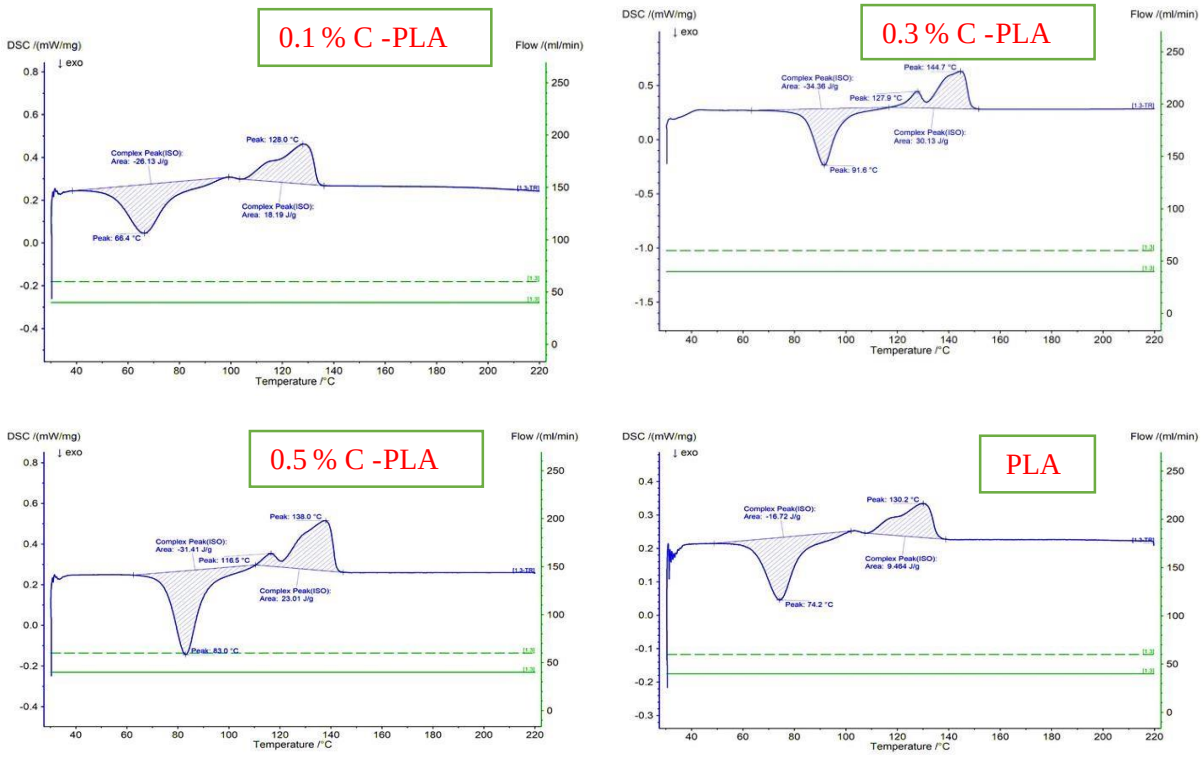


**Figure 6.** *DSC thermograms of neat PLA and PLA/cellulose bio-composites with different cellulose fiber loadings.*

**Table 2.** *Thermal parameters obtained from DSC analysis of PLA and PLA/cellulose bio-composites.*

| Sample | $T_g$ (°C) | $T_c$ (°C) | $\Delta H_c$ (J/g) | $T_m$ (°C) | $\Delta H_m$ (J/g) | $X_c$ (%) | % $X_c$ relative to neat PLA |
|---|---|---|---|---|---|---|---|
| PLA | 32.0 | 74.2 | -16.7 | 130.2 | 9.5 | 10.1 | 100.0 |
| PLA/0.1%C | 35.0 | 66.4 | -26.1 | 128.0 | 18.2 | 19.4 | 192.3 |
| PLA/0.3%C | 34.0 | 91.6 | -34.3 | 144.7 | 30.1 | 32.3 | 319.3 |
| PLA/0.5%C | 36.0 | 83.0 | -31.4 | 138.0 | 23.0 | 24.7 | 244.4 |

From the $T_g$ values shown in Table 2, it is evident that the glass transition temperature of the bio-composites exhibited only slight changes. The $T_g$ of the neat PLA was 32 °C, whereas reinforcement with cellulose fibers increased $T_g$ slightly to the range of 34–36 °C. Such minor variations in $T_g$ were

also reported in another study [28], which found that the $T_g$ of PLA/cellulose bio-composites did not differ significantly from that of neat PLA. Similar results were also documented in another published research [29], which explained that glass transition is a complex phenomenon governed by multiple factors, including intermolecular interactions, steric effects, chain flexibility, molecular weight, branching, and crosslinking density. Due to the relatively low cellulose content in the present study, only a small fraction of PLA chain mobility was restricted by the presence of the cellulose filler.

In contrast, the crystallization temperature ($T_c$) displayed more noticeable changes. Tc decreased upon the addition of 0.1% cellulose, increased at 0.3% cellulose, and decreased again at 0.5% cellulose. The crystallinity ($X_c$) of all cellulose-reinforced bio-composite increased compared with neat PLA, with the highest degree of crystallinity (32.3%) observed in the PLA/0.3% cellulose. This behavior indicates that cellulose may act as a nucleating agent, facilitating crystallization at lower temperatures and enhancing the overall crystallinity of PLA [30-32]. The high crystallinity observed at 0.3% cellulose loading can be attributed to well-dispersed cellulose fibers within the PLA matrix, which increased crystal density, improved crystal size distribution, and promoted nucleation, thereby favoring crystallization. However, at higher cellulose loading (0.5%), crystallinity decreased, likely due to fiber agglomeration that restricted PLA chain mobility and hindered crystal growth.

Regarding melting behavior, the DSC thermograms of all samples exhibited two melting endotherms. The first melting peak ($T_{m1}$, at lower temperature) and the second melting peak ($T_{m2}$, at higher temperature) were observed. The lower temperature melting peak ($T_{m1}$) may correspond to the melting of imperfect crystallites or small lamellae within the bio-composites. Among the tested bio-composites, the PLA/0.3% cellulose sample exhibited the highest melting temperature, further supporting its enhanced crystallinity.

### *3.7. Mechanical Properties Analysis*

**Table 3.** *Mechanical properties of neat PLA and PLA reinforced with different cellulose loadings.*

| Sample | Tensile strength (MPa) | Elongation at break (%) | Young's modulus (MPa) |
|---|---|---|---|
| PLA | 51.17±0.19 | 5.23±1.31 | 1811.18±5.17 |
| PLA/0.1%C | 34.24±2.95 | 3.45±0.91 | 627.6±81.12 |
| PLA/0.3%C | 30.14±1.92 | 2.16±1.49 | 671.15±69.22 |
| PLA/0.5%C | 40.31±9.27 | 4.63±1.82 | 712.29±72.82 |

Table 3 summarizes the mechanical properties of PLA reinforced with different cellulose loadings. The neat PLA exhibited a tensile strength of 51.17 ± 0.19 MPa, an elongation at break of 5.23 ± 1.31%, and a Young's modulus of 1811.18 ± 5.17 MPa. Upon incorporation of cellulose at loading ranging from 0.1% to 0.5%, the mechanical performance of the bio-composites decreased compared to that of neat PLA. This reduction may be attributed to the agglomeration of cellulose fibers within the PLA matrix, which weakens interfacial adhesion between the filler and the polymer, thereby impairing stress transfer efficiency [33].

### *3.8. Water Absorption Capacity*

**Table 4.** *Water absorption of neat PLA and PLA reinforced with different cellulose concentrations.*

| Sample | PLA | PLA/0.1%C | PLA/0.3%C | PLA/0.5%C |
|---|---|---|---|---|
| Water absorption after 24 hours (%) | 54.3±2.8 | 115.4±3.1 | 138±10.1 | 312.3±24.4 |

Table 4 presents the water absorption capacity of PLA bio-composites containing different cellulose loadings after 24 h immersion. The incorporation of cellulose into the PLA matrix significantly increased the water uptake of the bio-composites. The PLA/0.1%C bio-composite exhibited a twofold increase in water absorption compared with neat PLA, reaching 115.4 ± 3.1%. A further increase was observed for the PLA/0.3%C bio-composite, which reached 138.6 ± 10.1%. The highest water

absorption was recorded for the PLA/0.5%C bio-composite, with a value of 312.3 ± 24.4%, approximately 5.7 times greater than that of neat PLA.

This behavior can be explained by the hydrophilic nature of cellulose, which contains abundant hydroxyl groups capable of forming hydrogen bonds with water molecules. Water penetrates through the bio-composite surface and diffuses into both the PLA matrix and the cellulose fibers. Since cellulose exhibits high water absorption capacity, its presence accelerates the diffusion process. Therefore, as the cellulose content increases, the overall water absorption capacity of the bio-composites tends to rise accordingly [34].

## 4. Conclusions

In this study, cellulose fibers were successfully extracted from sugarcane bagasse and employed as a reinforcing agent for PLA-based bio-composites. SEM analysis revealed that the extracted cellulose fibers possessed smooth surfaces and were relatively well dispersed in the PLA matrix. FTIR results confirmed that the characteristic chemical structure of cellulose was preserved after chemical treatment. XRD analysis identified a crystallinity index of 63.71% for the cellulose fibers, indicating the effective removal of amorphous components. TGA analysis demonstrated three characteristic stages of thermal degradation of obtained cellulose fibers. Mechanical testing showed that the bio-composites reinforced with cellulose fibers at different loadings exhibited a decrease in mechanical properties compared to the unreinforced PLA bio-composites. The research results confirm the ability to utilize sugarcane bagasse as an abundant source of agricultural by-products to produce biofiber materials used as a filler for the fabrication of bio-composites based on environmentally friendly polymer (PLA). The fabricated bio-composites present great potential for application as a sustainable and environmentally friendly agricultural mulch film replacing the conventional petroleum-based polyethylene agricultural mulch film.

## Acknowledgments

We would like to thank Ho Chi Minh City University of Technology and Education for the financial support. This work belongs to project grant no. SV2025-35, funded by Ho Chi Minh City University of Technology and Education, Vietnam.

## Conflict of Interest

The authors declare no conflict of interest.

## Data Availability Statement

The data that support the findings of this study are available from the corresponding author upon reasonable request.

## REFERENCES

[1] A. M. Panicker, K. A. Rajesh, and T. O. Varghese, "Mixed morphology nanocrystalline cellulose from sugarcane bagasse fibers/poly(lactic acid) nanocomposite films: synthesis, fabrication and characterization," *Iranian Polymer Journal*, vol. 26, no. 2, pp. 125-136, 2017.

[2] M. Jonoobi, J. Harun, A. P. Mathew, and K. Oksman, "Mechanical properties of cellulose nanofiber (CNF) reinforced polylactic acid (PLA) prepared by twin screw extrusion," *Composites Science and Technology*, vol. 70, no. 12, pp. 1742-1747, 2010.

[3] C. G. Li, W. G. Peng, Y. X. Li, P. F. Xu, W. Tian, and R. Zhang, "Thermal and mechanical properties of bagasse microcrystalline cellulose reinforced PLA composites," *Advanced Materials Research*, vol. 284, pp. 1786-1789, 2011.

[4] I. Armentano *et al.*, "Multifunctional nanostructured PLA materials for packaging and tissue engineering," *Progress in Polymer Science*, vol. 38, no. 10-11, pp. 1720-1747, 2013.

[5] M. A. S. A. Samir, F. Alloin, and A. Dufresne, "Review of recent research into cellulosic whiskers, their properties and their application in nanocomposite field," *Biomacromolecules*, vol. 6, no. 2, pp. 612-626, 2005.

[6] N. D. Vu, H. T. Tran, N. D. Bui, C. D. Vu, and H. V. Nguyen, "Lignin and Cellulose Extraction from Vietnam's Rice Straw Using Ultrasound-Assisted Alkaline Treatment Method," vol. 2017, no. 1, p. 1063695, 2017.

[7] D. Michel, B. Bachelier, J. Y. Drean, and O. Harzallah, "Preparation of cellulosic fibers from sugarcane for textile use," in *Conference Papers in Science*, 2013, vol. 2013, p. 651787: Wiley Online Library.

[8] R. Z. Khoo, W. S. Chow, and H. Ismail, "Sugarcane bagasse fiber and its cellulose nanocrystals for polymer reinforcement and heavy metal adsorbent: a review," *Cellulose*, vol. 25, no. 8, pp. 4303-4330, 2018.

[9] G. T. Melesse, F. G. Hone, and M. A. Mekonnen, "Extraction of cellulose from sugarcane bagasse optimization and characterization," *Advances in materials science and engineering*, vol. 2022, no. 1, p. 1712207, 2022.

[10] B. Bahrami, T. Behzad, A. Zamani, P. Heidarian, and B. N. Nasrabadi, "Optimal design of ozone bleaching parameters to approach cellulose nanofibers extraction from sugarcane bagasse fibers," *Journal of Polymers and the Environment*, vol. 26, no. 10, pp. 4085-4094, 2018.

[11] M. A. Mahmud and F. R. Anannya, "Sugarcane bagasse-A source of cellulosic fiber for diverse applications," *Heliyon*, vol. 7, no. 8, 2021.
[12] R. K. Gond and M. K. Gupta, "Development and characterization of PLA-based green nanocomposite films for sustainable packaging applications," *Journal of Natural Fibers*, vol. 19, no. 17, pp. 15738-15750, 2022.
[13] W. Rasri, V. T. Thu, A. Corpuz, and L. T. Nguyen, "Preparation and characterization of cellulose nanocrystals from corncob via ionic liquid [Bmim][HSO 4] hydrolysis: Effects of major process conditions on dimensions of the product," *RSC advances*, vol. 13, no. 28, pp. 19020-19029, 2023.
[14] C. A. Saputri, F. A. Julyatmojo, M. Febrina, M. Mahardika, and S. Maulana, "Characteristics of bioplastics prepared from cassava starch reinforced with banana bunch cellulose at various concentrations," vol. 1309, p. 012006: IOP Publishing.
[15] Y. H. Feng *et al.*, "Characteristics and environmentally friendly extraction of cellulose nanofibrils from sugarcane bagasse," *Industrial Crops and Products*, vol. 111, pp. 285-291, 2018.
[16] A. A. Mubarak, R. A. Ilyas, N. Ngadi, A. H. Nordin, and M. F. M. Alkbir, "Isolation and characterization of cellulose from sugarcane bagasse fiber (Saccharum officinarum) via delignification and mercerization treatment using response surface modeling (RSM)," *Biomass Conversion and Biorefinery*, pp. 1-15, 2024.
[17] M. Y. Foroushani, A. Y. Foroushani, and H. Yarahmadi, "Analysis of mechanical techniques in extracting cellulose fibers from sugarcane bagasse," *Biomass Conversion and Biorefinery*, pp. 1-14, 2025.
[18] M. K. Nacos *et al.*, "Kenaf xylan–A source of biologically active acidic oligosaccharides," *Carbohydrate polymers*, vol. 66, no. 1, pp. 126-134, 2006.
[19] R. M. Salim, J. Asik, and M. S. Sarjadi, "Chemical functional groups of extractives, cellulose and lignin extracted from native Leucaena leucocephala bark," *Wood Science and Technology*, vol. 55, no. 2, pp. 295-313, 2021.
[20] J. I. Morán, V. A. Alvarez, V. P. Cyras, and A. Vázquez, "Extraction of cellulose and preparation of nanocellulose from sisal fibers," *Cellulose*, vol. 15, no. 1, pp. 149-159, 2008.
[21] N. Terinte, R. Ibbett, and K. C. Schuster, "Overview on native cellulose and microcrystalline cellulose I structure studied by X-ray diffraction (WAXD): Comparison between measurement techniques," *Lenzinger Berichte*, vol. 89, no. 1, pp. 118-131, 2011.
[22] M. Li, L. J. Wang, D. Li, Y. L. Cheng, and B. Adhikari, "Preparation and characterization of cellulose nanofibers from de-pectinated sugar beet pulp," *Carbohydrate Polymers*, vol. 102, pp. 136-143, 2014.
[23] T. A. Adewole, H. A. Hassan, O. O. Daramola, and B. Bakeer, "Effect of chemical treatment on the tensile, and morphological properties of date palm/bagasse and hybrid reinforced polyester matrix composites," *Scientific African*, p. e02849, 2025.
[24] H. S. Kassa, S. A. Jabasingh, S. A. Mohammed, S. Y. Baek, and S. Y. Park, "Extraction and characterization of cellulose nanocrystals from anchote (Coccinia abyssinica) bagasse," *Macromolecular Research*, vol. 30, no. 11, pp. 776-782, 2022.
[25] M. Kowalczyk, E. Piorkowska, P. Kulpinski, and M. Pracella, "Mechanical and thermal properties of PLA composites with cellulose nanofibers and standard size fibers," *Composites Part A: Applied Science and Manufacturing*, vol. 42, no. 10, pp. 1509-1514, 2011.
[26] F. Mosley, "Biodegradable polylactic acid cellulose nanocomposites," 2018.
[27] H. Kyutoku, N. Maeda, H. Sakamoto, H. Nishimura, and K. Yamada, "Effect of surface treatment of cellulose fiber (CF) on durability of PLA/CF bio-composites," *Carbohydrate polymers*, vol. 203, pp. 95-102, 2019.
[28] I. Spiridon, R. N. Darie, and H. Kangas, "Influence of fiber modifications on PLA/fiber composites. Behavior to accelerated weathering," *Composites Part B: Engineering*, vol. 92, pp. 19-27, 2016.
[29] A. N. Frone, S. Berlioz, J. F. Chailan, and D. M. Panaitescu, "Morphology and thermal properties of PLA–cellulose nanofibers composites," *Carbohydrate polymers*, vol. 91, no. 1, pp. 377-384, 2013.
[30] S. O. Han *et al.*, "Understanding the reinforcing mechanisms in kenaf fiber/PLA and kenaf fiber/PP composites: A comparative study," *International Journal of Polymer Science*, vol. 2012, no. 1, p. 679252, 2012.
[31] B. H. Lee, H. S. Kim, S. Lee, H. J. Kim, and J. R. Dorgan, "Bio-composites of kenaf fibers in polylactide: Role of improved interfacial adhesion in the carding process," *Composites Science and Technology*, vol. 69, no. 15-16, pp. 2573-2579, 2009.
[32] S. M. Luz, J. Del Tio, G. J. M. Rocha, A. R. Gonçalves, and A. P. Del'Arco Jr, "Cellulose and cellulignin from sugarcane bagasse reinforced polypropylene composites: Effect of acetylation on mechanical and thermal properties," *Composites Part A: Applied Science and Manufacturing*, vol. 39, no. 9, pp. 1362-1369, 2008.
[33] K. Jin, Y. Tang, X. Zhu, and Y. Zhou, "Polylactic acid based biocomposite films reinforced with silanized nanocrystalline cellulose," *International Journal of Biological Macromolecules*, vol. 162, pp. 1109-1117, 2020.
[34] B. S. Ndazi and S. Karlsson, "Characterization of hydrolytic degradation of polylactic acid/rice hulls composites in water at different temperatures," *Express Polymer Letters*, vol. 5, no. 2, 2011.

**Nguyen Hong Nhu Pham** studying Materials Technology at Ho Chi Minh City of Technology and Education.
Email: 21130086@student.hcmute.edu.vn. ORCID: https://orcid.org/0009-0002-6514-4518

**Van Tai Pham** studying Materials Technology at Ho Chi Minh City of Technology and Education.
Email: 21130096@student.hcmute.edu.vn. ORCID: https://orcid.org/0009-0009-1247-5955

**Phuong Dong Bui** received his Bachelor Engineering degree in Materials Technology from Ho Chi Minh City University of Technology and Education in 2024.
Email: 20130020@student.hcmute.edu.vn. ORCID: https://orcid.org/0009-0007-5228-4980

**Thanh Huy Nguyen** received his Bachelor Engineering degree in Materials Technology from Ho Chi Minh City University of Technology and Education in 2023.
Email: huynt171201@gmail.com. ORCID: https://orcid.org/0009-0004-1110-286X

**Bui Anh Duy Nguyen** received his Bachelor Engineering degree in Materials Technology from Ho Chi Minh City University of Technology and Education in 2023.
Email: anhduy240901@gmail.com. ORCID: https://orcid.org/0009-0004-6535-8027

**Thi Thuy Giang Bach** received her Bachelor Engineering degree in Chemical Engineering Technology from Nong Lam University Ho Chi Minh City in 2022.
Email: bachthuygiang301299@gmail.com. ORCID: https://orcid.org/0009-0008-5181-0122

**Chi Thanh Nguyen** received his Bachelor degree in Materials Science from Ho Chi Minh City University of Sciences, Viet Nam and the Ph.D. degree in Polymer Engineering from Suranaree University of Technology, Thailand. He is currently a lecturer at Ho Chi Minh City University of Technology and Education, Viet Nam.
Email: thanhnc@hcmute.edu.vn. ORCID: https://orcid.org/0000-0003-3638-9903